Quantum Reaction Dynamics of Heavy−Light−Heavy Systems: Reduction of the Number of Potential Curves and Transitions at Avoided Crossings

Katsuyuki Nobusada, Oleg I. Tolstikhin,† and Hiroki Nakamura*

Division of Theoretical Studies, Institute for Molecular Science, Myodaiji, Okazaki 444, Japan

Received: April 20, 1998; In Final Form: July 6, 1998

Two decoupling procedures are proposed within the framework of the hyperspherical coordinate approach in order to reduce the number of states in the close-coupling calculations and to clarify the reaction mechanisms. Sharply avoided adiabatic states are diabatically connected and relabeled without any diabatic coupling there. This is named diabatic decoupling and is useful for decoupling two manifolds of states belonging to different categories. Furthermore, the number of states is reduced in such a way that only a limited number of adjacent adiabatic states are taken into account in the close-coupling calculations for each relevant state. This is called adiabatic decoupling scheme. These reductions of the number of states enable us to analyze reactions in terms of nonadiabatic transitions at avoided crossings among the small number of adiabatic potential curves. The method is applied to $O(^3P) + HCl \rightarrow OH + Cl$ and $Cl + HCl \rightarrow HCl + Cl$. The idea of vibrationally nonadiabatic transitions at avoided crossings together with the concept of potential ridge introduced in our previous paper can untangle the congested potential curves and clarify reaction mechanisms.

1. Introduction

Recent progress in theoretical studies of quantum dynamics of chemical reactions is remarkable in both time-independent and time-dependent treatments.[1−3] Not only triatomic but also tetraatomic systems can be accurately analyzed. In general, the time-independent treatment has more advantages for clarifying the reaction mechanisms. On the other hand the time-dependent one is more powerful for attacking large systems. In these theoretical studies of chemical reactions, there are two important aspects other than evaluating the dynamics of each particular reaction process. One is to elucidate general reaction mechanisms as much as possible and to conceptualize them. The other is to improve numerical efficiency in terms of both CPU capability and algorithmic innovation. Needless to say, both are important not only for comprehending the reaction mechanisms of triatomic systems but also for challenging larger reaction systems. In the present series of work, emphasis is placed on qualitative understanding of the reaction mechanisms in heavy−light−heavy (HLH) systems.

The light atom transfer reactions in HLH systems have attracted much attention theoretically, since they are not only important in various physicochemical processes but also intriguing in themselves because of the various quantum mechanical effects. Quantum mechanical as well as semiclassical calculations and analyses have been carried out for the various three-dimensional (3D) HLH reactions so far.[4−10] Recently, we have developed a new theory[11,12] for light atom transfer reactions with use of the new coordinate system, i.e., the hyperspherical elliptic coordinates.[13] This coordinate system together with the methods of the slow/smooth-variable-discretization (SVD)[14] and the discrete-variable-representation (DVR)[15] improves the numerical efficiency very much and enables us to quantum mechanically accurately deal with even vibrationally nonadiabatic chemical reactions. Furthermore, with an effective use of the vibrational adiabaticity this theory turns out to be very powerful for clarifying the reaction mechanisms of 3D HLH systems in terms of nonadiabatic transitions at some important avoided crossings.[12] The role of avoided crossings has been discussed by Kubach and co-workers using the Born−Oppenheimer separation approximation.[6] In our treatment based on the new coordinate system, to pick up the important avoided crossings, the concept of potential ridge,[16] which can be clearly defined and has been proved to be useful for clarifying the dynamics in collinear reactions,[17,18] has been successfully generalized to 3D reactions.[12]

In this paper we further pursue the above-mentioned idea and try to reduce the number of states in the close coupling calculations and to clarify the mechanisms. This is based on the belief that not all of the states are needed to obtain converged scattering matrix elements for any specified initial state. Such reduction of the number of states would enable us not only to further improve numerical efficiency but also to accelerate the understanding of reaction mechanisms. Especially, the diabatic decoupling scheme is quite useful when two groups of curves corresponding to two different configurations separated by a potential barrier depict sharp avoided crossings. In the previous paper (referred to as I),[12] we discussed only a small number of reactive transitions predominated by the avoided crossings along the potential ridge line. Here, we try to get further insights into the reaction mechanisms in terms of nonadiabatic transitions at avoided crossings not only along the potential ridge line but also on the left side of it. The idea is applied to the same system ($O + HCl$) as in I and also to the reaction $Cl + HCl \rightarrow HCl + Cl$. The first one represents an example of thermoneutral HLH reactions, and the second represents a symmetric HLH reaction. Some specific feature about the symmetric reaction system will also be discussed. An asymmetric endo- or exothermic HLH reaction will be discussed in a future publication. In most of the cases we use the LEPS potential energy surfaces (PES), which usually cannot represent realistic ones. It is not a primary purpose here, however, to directly compare with any experi-

† Permanent address: P. N. Lebedev Physical Institute, Russian Academy of Sciences, Moscow, Russia.

10.1021/jp981920v CCC: $15.00
Published on Web 11/03/1998

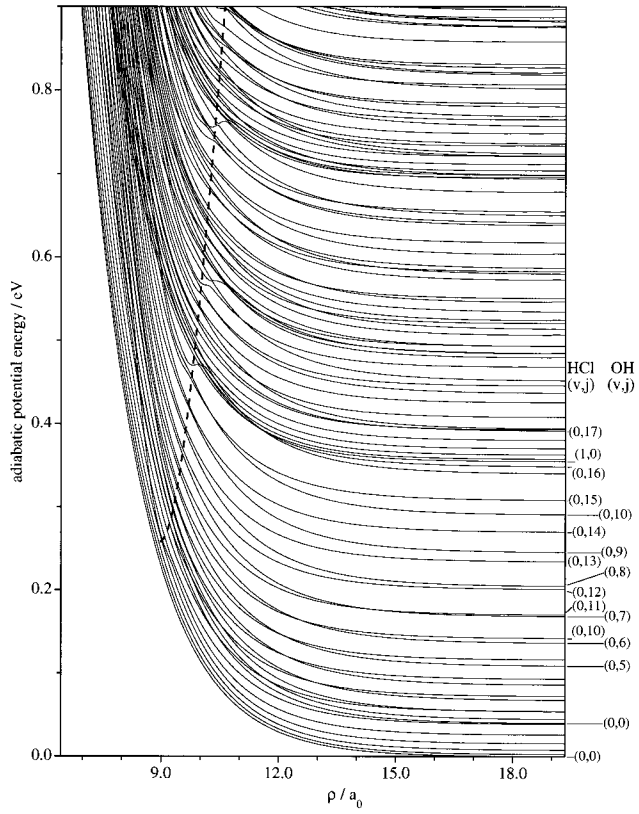

Figure 1. Adiabatic potential curves as a function of hyperradius ρ in the case of LEPS of OHCl. The energy is measured from the ground state ($v_i = j_i = 0$) of the reactant HCl. The dash line represents the $n_\xi = 0$ ridge line. The numbers in brackets at the right edge indicate the vibrational and rotational quantum numbers of HCl and OH.

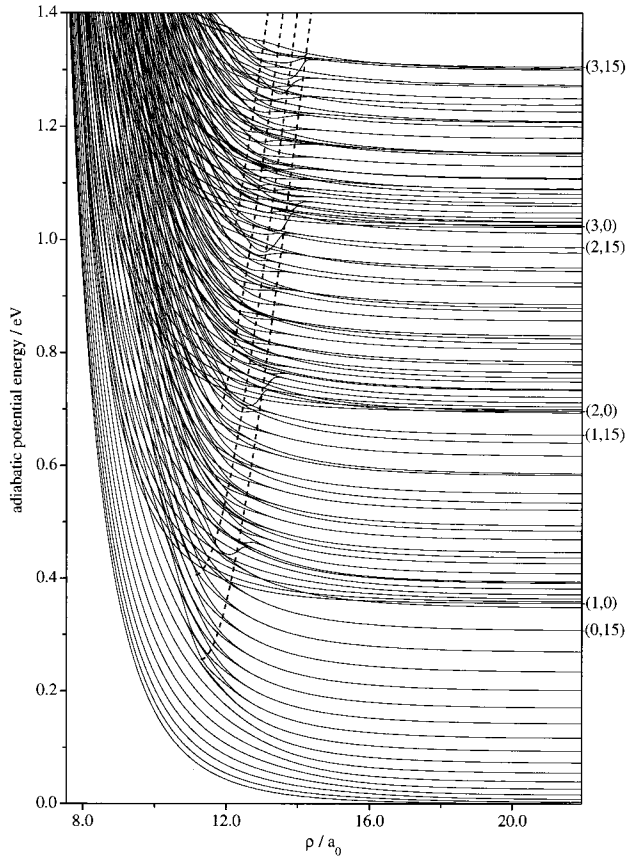

Figure 2. Adiabatic potential curves as a function of hyperradius ρ in the case of LEPS of ClHCl. The energy is measured from the ground state ($v_i = j_i = 0$) of HCl. The dash lines represent the $n_\xi = 0$, 1, 2, and 3 ridge lines. The numbers in brackets at the right edge indicate the representative vibrational and rotational quantum numbers of HCl.

mental results. The concept of nonadiabatic transitions at avoided crossings established in the present series of work is not just restricted to LEPS PES but should be general and useful to comprehend reaction mechanisms.

This paper is organized as follows. In the next section, we briefly summarize the basic equations in the hyperspherical elliptic coordinate approach. Two types of decoupling schemes, diabatic and adiabatic ones, are introduced and applied to the two reaction systems in section 3. Reaction mechanisms are elucidated in terms of nonadiabatic transitions at avoided crossings in section 4. Some particular feature about potential curve splittings in the symmetric system is discussed in section 5. Concluding remarks are provided in section 6.

2. Basic Equations in the Hyperspherical Elliptic Coordinate Approach

Since the hyperspherical elliptic coordinate approach has been previously described in detail,[11,12] here we give only its brief outline. The coordinate system consists of the hyperradius ρ and the hyperspherical elliptic angles (ξ, η) to parametrize the hypersphere. With use of these coordinates, the Schrödinger equation for J (total angular momentum quantum number) $= 0$ is given by

$$[K(\rho) + H_{ad}(\xi,\eta;\rho) - \mu\rho^2 E]\Psi(\rho,\xi,\eta) = 0 \qquad (1)$$

where $K(\rho)$ represents the kinetic energy with respect to ρ, H_{ad} is the adiabatic Hamiltonian defined at fixed ρ, which is composed of the angular kinetic energy and the interaction potential, μ is the characteristic mass, and E is the total energy measured from the ground rovibrational state of the reactant HCl. The adiabatic potentials $U_\nu(\rho)$ and the channel eigenfunctions $\Phi_\nu(\xi,\eta;\rho)$ are obtained by solving the following eigenvalue problem:

$$[H_{ad}(\xi,\eta;\rho) - \mu\rho^2 U_\nu(\rho)]\Phi_\nu(\xi,\eta;\rho) = 0 \qquad (2)$$

where ν indicates the adiabatic channel number. This is a mathematically two-dimensional (2D) eigenvalue problem and is efficiently solved by taking advantage of the good separability of the hyperspherical elliptic coordinates ξ and η in the HLH systems.[11,12] Equation 2 is first solved with respect to the ξ-motion, which well represents the vibrational motion of both reactant and product, and then with respect to the η-motion. After solving the eigenvalue problem with respect to ξ, we obtain the vibrationally adiabatic potentials for each vibrational state n_ξ.[12] The potential ridge line for each n_ξ is drawn as a function of ρ by projecting the barrier top of the corresponding vibrationally adiabatic potential. The role of the potential ridge has been fully discussed in the paper I.

To solve eq 1, we use the SVD method developed by Tolstikhin et al.[14] and the solution is expanded as

$$\Psi_n(\rho,\xi,\eta) = \sum_{i=1}\sum_{\nu=1} C^n_{i\nu}\pi_i(\rho)\Phi_\nu(\xi,\eta;\rho_i) \qquad (3)$$

where $\pi_i(\rho)$ is the DVR basis function and ρ_i is the quadrature point. Substituting the expansion (eq 3) into eq 1, we obtain the following coupled differential equations:

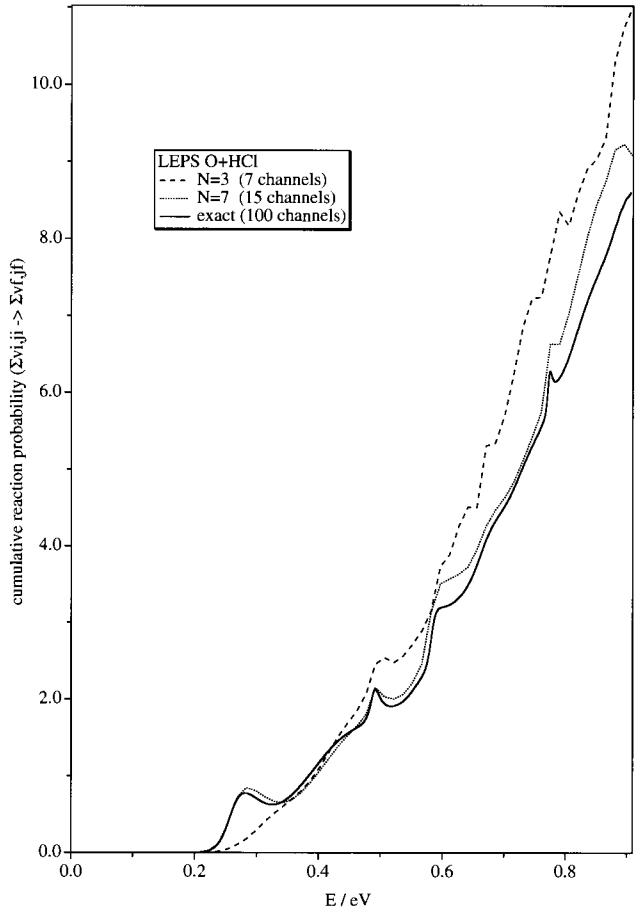

Figure 3. Total cumulative reaction probability $P(\sum_{v_i,j_i} \rightarrow \sum_{v_f,j_f})$ as a function of the total energy E measured from the ground state of the reactant in the case of LEPS of OHCl: (solid line) exact numerical result; (dash line) $N = 3$ decoupling calculation; (dotted line) $N = 7$ decoupling calculation.

$$\sum_{j=1}\sum_{\mu=1}(K_{ij}O_{i\nu,j\mu} + \mu\rho_i^2[U_\nu(\rho_i) - E_n]\delta_{ij}\delta_{\nu\mu})C_{j\mu}^n = 0 \quad (4)$$

where

$$K_{ij} = \int \pi_i(\rho)K(\rho)\pi_j(\rho)\,\mathrm{d}\rho \quad (5)$$

and $O_{i\nu,j\mu}$ is the overlap matrix at different quadrature points ρ_i and ρ_j given by

$$O_{i\nu,j\mu} = \langle\Phi_\nu(\xi,\eta;\rho_i)|\Phi_\mu(\xi,\eta;\rho_j)\rangle \quad (6)$$

The coefficients $C_{j\mu}^n$ obtained in each sector of ρ are propagated to the asymptotic region by using the **R** matrix propagation method.[19] After imposing a proper scattering boundary condition on $\Psi_n(\rho,\xi,\eta)$ in the asymptotic region, the scattering matrix is finally obtained.

3. Decoupling Scheme

A. Diabatic and Adiabatic Decoupling. The following two types of decoupling schemes are considered. One is the decoupling in adiabatic representation, and the other is the decoupling in diabatic representation. The former procedure is simple because the state labeling of $\Phi_\nu(\xi,\eta;\rho)$ is always adiabatic, i.e., in the order of increasing energy. This decoupling is carried out in such a way that $2N$ (N states higher and N states lower) adjacent potential curves are taken into account for each state. The off-diagonal overlap matrix elements outside this range are simply put equal to zero. On the other hand, the diabatic decoupling scheme is useful among sharply avoided states but is more laborious. In many instances adiabatic potentials have sharply avoided crossings that do not have any dynamical significance. In such a case it is better to relabel those adiabatic states diabatically and to put the diabatic interaction equal to zero, or the adiabatic overlap matrix element equal to unity. To do this, we introduce a certain criterion (CRT), and the above diabatic decoupling is carried out when the condition $O_{i\nu,j\mu} \geq$ CRT is satisfied. Applying this criterion to sharply avoided crossings, we obtain new potential curves in the diabatic representation. After relabeling the potential curves, we can further apply the above-mentioned adiabatic decoupling scheme. This diabatization is physically meaningful and useful when two groups of curves of different character have sharply avoided crossings. In paper I,[12] we demonstrated that avoided crossings that appear far to the right of the potential ridge line (see, for instance, Figures 5 and 6 of I) do not contribute to the reaction and that the system develops diabatically without nonadiabatic transitions there. In such a case, the diabatic decoupling is useful.

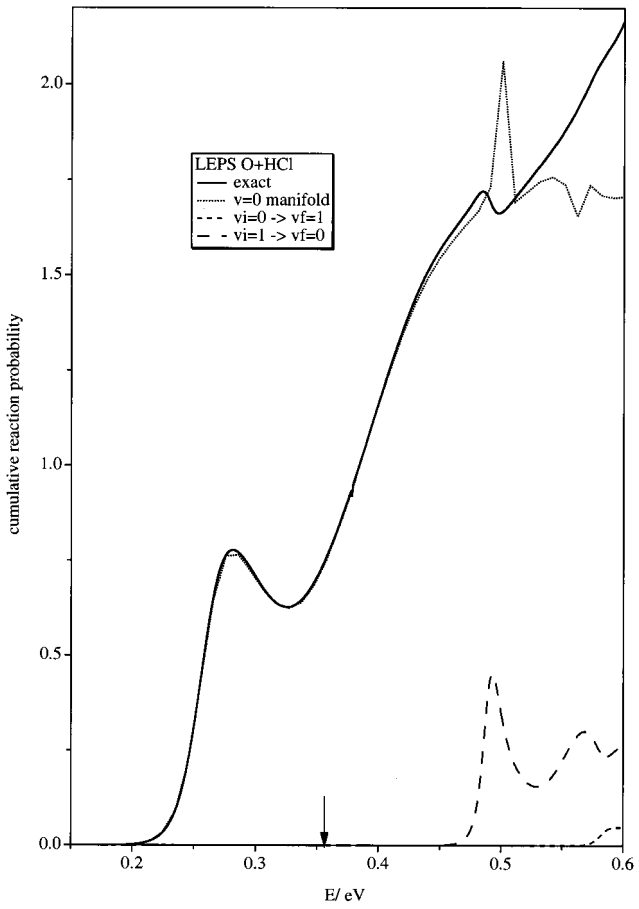

Figure 4. Vibrationally specified cumulative reaction probabilities as a function of the total energy E in the case of LEPS of OHCl: (solid line) exact numerical result for $(v_i = 0,\Sigma_{j_i}) \rightarrow (v_f = 0,\Sigma_{j_f})$; (dotted lines) exact numerical results for $(v_i = 0,\Sigma_{j_i}) \rightarrow (v_f = 1,\Sigma_{j_f})$ and $(v_i = 1,\Sigma_{j_i}) \rightarrow (v_f = 0,\Sigma_{j_f})$; (dash line) the same as the solid line with the $v = 1$ manifold disregarded.

The above decoupling methods are applied to an example of the thermoneutral HLH reactions $O(^3P) + HCl \rightarrow OH + Cl$ and a symmetric HLH reaction $Cl + HCl \rightarrow HCl + Cl$. Figures 1 and 2 show the corresponding adiabatic potential energy diagrams together with the vibrationally adiabatic ridge lines (dash line) based on the LEPS potential energy surfaces (PES)

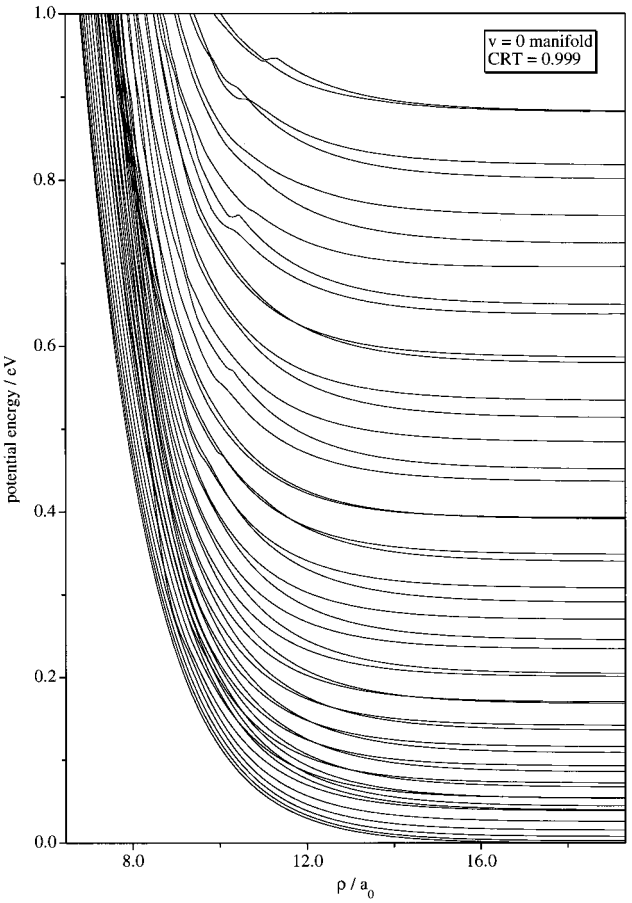

Figure 5. Adiabatic potential curves of the $v = 0$ manifold based on the overlap matrix criterion CRT = 0.999 for LEPS of OHCl.

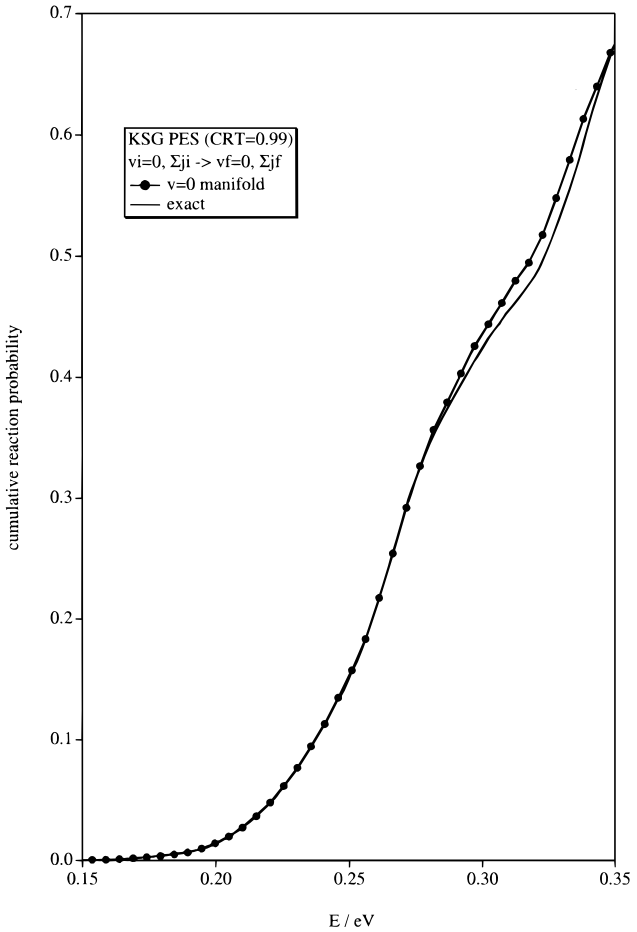

Figure 6. Vibrationally specified cumulative reaction probabilities as a function of the total energy E in the case of the KSG surface: (solid line) exact numerical result for $(v_i = 0,\sum_{ji}) \rightarrow (v_f = 0,\sum_{jf})$; (solid line with closed circles) same as the solid line with the $v = 1$ manifold disregarded.

for O + HCl (Figure 1)[20] and for Cl + HCl (Figure 2).[21] We have also used the KSG potential for O + HCl.[5]

B. Cumulative Reaction Probabilities. Figure 3 shows the total cumulative reaction probabilities $P(\sum v_i,j_i \rightarrow \sum v_f,j_f)$ obtained by the fully coupled exact numerical calculations and also by the two adiabatic decoupling calculations ($N = 3$ and 7) in the case of LEPS of OHCl. Roughly speaking, this corresponds to $N \sim N + 1$ reaction channels and $N + 1 \sim N$ excitation channels. The $N = 7$ decoupling calculation (dotted line) sufficiently reproduces the exact result in the wide energy range. Even the $N = 3$ decoupling calculation (dash line) works quite well, although the small peak at low energy ($0.22 \lesssim E \lesssim 0.32$ eV) is not reproduced. These results are rather amazing and encouraging when we look at the congestion of states especially at high energies $E \gtrsim 0.6$ eV.

At energies slightly higher than the $v = 1$ threshold ($\sim$0.36 eV) in the present OHCl system, there appear sharply avoided crossings between the $v = 0$ and $v = 1$ manifolds even in the reaction zone, i.e., the intermediate ρ region. Here, the diabatic decoupling scheme is useful for separating these two manifolds. Figure 4 shows the vibrationally adiabatic cumulative reaction probability ($v_i = 0,\sum j_i \rightarrow v_f = 0,\sum j_f$) (solid line) and the vibrationally nonadiabatic cumulative reaction probabilities ($v_i = 1(0),\sum j_i \rightarrow v_f = 0(1),\sum j_f$) (dash lines). The arrow in the figure indicates the $v = 1$ threshold. Even above the $v = 1$ threshold, the $v = 1$ states are not dynamically accessible up to $E \approx 0.45$ eV. Thus, we expect that the vibrationally adiabatic cumulative reaction probability can be evaluated accurately only within the $v = 0$ manifold at $E \lesssim 0.45$ eV. To confirm this expectation, we carried out the diabatic decoupling calculation. Figure 5 shows the $v = 0$ diabatic potential energy curves corresponding to CRT = 0.999. Compared with Figure 1, a large number of potential curves are omitted and it becomes easier to analyze the dynamics. Using this $v = 0$ diabatic manifold, we have evaluated the cumulative reaction probability ($v_i = 0,\sum j_i \rightarrow v_f = 0,\sum j_f$), which is shown in Figure 4 by the dotted line. The result nicely reproduces the exact one up to $E \approx 0.48$ eV, demonstrating the effectiveness of the present diabatic decoupling scheme. The peak appearing in the dotted line at $E \approx 0.5$ eV is simply due to the neglect of the $v = 1$ manifold.

For the O(^{3}P) + HCl system another PES named KSG is available. This is based on the ab initio calculations but, unfortunately, contains two rather crucial artifacts. Thus, this PES cannot represent a realistic potential as pointed out previously.[6,8,11,22] This is actually a reason that we have used the LEPS PES. It should be noted that the methodology of reducing the number of states and the idea of clarifying reaction mechanisms discussed in the present paper should work well in general for HLH reactions. However, to demonstrate the generality of the method, we have applied the diabatic decoupling method to the KSG PES at $E \lesssim 0.35$ eV and removed the $v = 1$ manifold. Figure 6 shows the vibrationally specified cumulative reaction probabilities ($v_i = 0,\sum j_i \rightarrow v_f = 0,\sum j_f$). The decoupling of the $v = 1$ manifold works correctly. We did not try this decoupling at higher energies simply because the artifact of the KSG surface gives unnatural features and prevents state identification even at large ρ. Although we do not show any

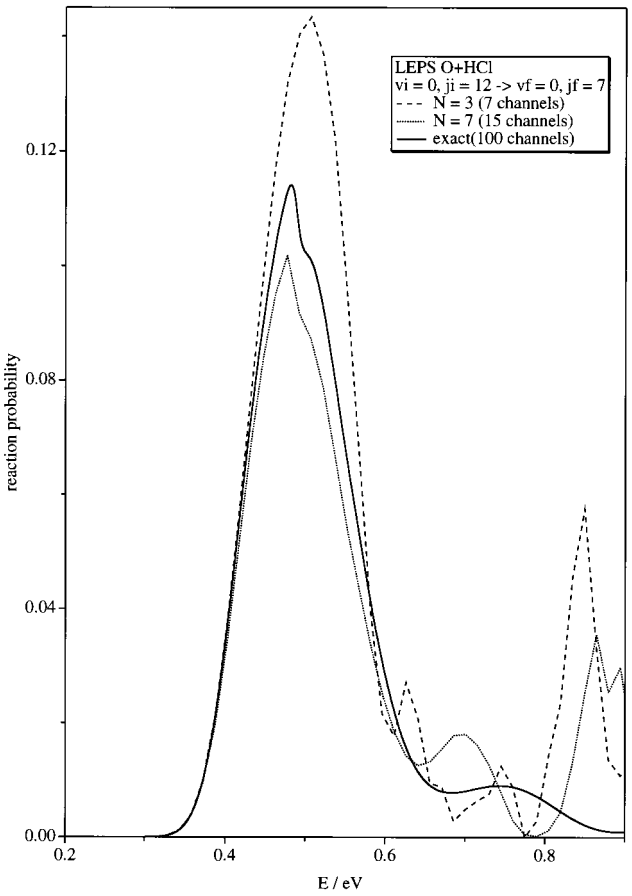

Figure 7. State-to-state reaction probability as a function of the total energy E for O + HCl($v_i = 0$, $j_i = 12$) → OH($v_f = 0$, $j_f = 7$) + Cl in the case of LEPS: (solid line) exact numerical result; (dash line) $N = 3$ decoupling calculation; (dotted line) $N = 7$ decoupling calculation.

figures, the adiabatic decoupling with $N = 10-15$ nicely reproduces the total cumulative reaction probability up to $E \approx 0.7$ eV.

C. State-to-State Reaction. Figure 7 shows results of the same adiabatic decoupling calculations as in Figure 3 but for the state-to-state ($v_i = 0$, $j_i = 12 \rightarrow v_f = 0$, $j_f = 7$) reaction. Even the $N = 3$ decoupling scheme seems to be qualitatively good enough for state-to-state processes at least at energies $E \lesssim 0.6$ eV.

Figure 8 shows results of the adiabatic decoupling ($N = 3$ and 10) for the reaction Cl + HCl($v_i = 0$, $j_i = 15$) → HCl($v_f = 0$, $j_f = 15$) + Cl and Cl + HCl($v_i = 0$, $j_i = 20$) → HCl($v_f = 1$, $j_f = 12$) + Cl. The first peaks are nicely reproduced by the decoupling. Even the $N = 3$ decoupling gives qualitatively correct results.

The results presented above confirm that reactions in the HLH systems are governed by a rather small number of states, and thus, the mechanisms may be comprehended in terms of vibrationally nonadiabatic transitions among these potential curves.

4. Reaction Mechanisms: Nonadiabatic Transitions at Avoided Crossings

In the previous section, we have confirmed that several potential curves adjacent to a specified initial channel predominate the reaction dynamics. In other words, it is sufficient to consider only several adjacent curves, and actually, the major reaction mechanisms can be clarified in terms of avoided

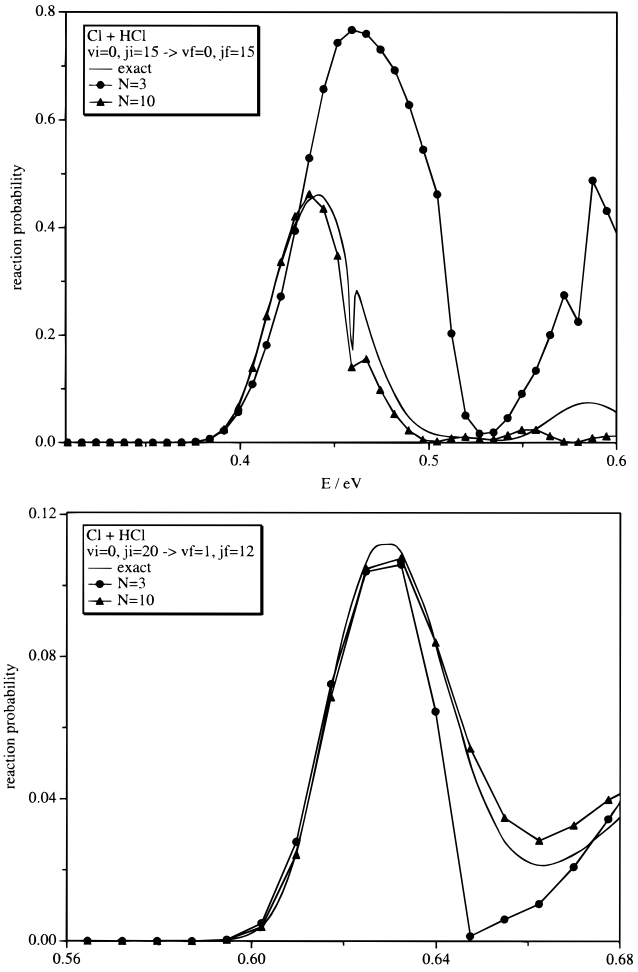

Figure 8. State-to-state reaction probability as a function of the total energy E for Cl + HCl($v_i = 0$, $j_i = 15$) → HCl($v_f = 0$, $j_f = 15$) + Cl (upper panel) and Cl + HCl($v_i = 0$, $j_i = 20$) → HCl($v_f = 1$, $j_f = 12$) + Cl (lower panel): (solid line) exact numerical result; (closed circles) $N = 3$ decoupling calculation; (closed triangles) $N = 10$ decoupling calculation.

crossings among them. This will be demonstrated below for the two reaction systems O + HCl and Cl + HCl.

A. O + HCl. As a representative case of this reaction on the LEPS surface, we take the state-to-state reactive transitions from $j_i = 12$. To depict the avoided crossings around this state much more clearly, the adiabatic potential energy curves measured from this state, i.e., $U_v(\rho) - U_{v_i=0,j_i=12}(\rho)$, are plotted in Figure 9. Some important avoided crossings are labeled by alphabetical characters.

Now, we focus our attention on the state-to-state reactions from $j_i = 12$ in the energy range 0.3 eV $\lesssim E \lesssim$ 0.7 eV. The results are shown in Figure 10a. The curve of $j_f = 7$ gives the maximum peak, and that of $j_f = 6$ presents the second maximum peak. The reaction $j_i = 12 \rightarrow j_f = 7$ in this energy range must be mainly determined by the nonadiabatic transition at the avoided crossing labeled as B. For the reaction of $j_i = 12 \rightarrow j_f = 6$ we may expect the following mechanisms. One is a transition through an inelastic channel, i.e., $j_i = 12 \rightarrow j_i = 11 \rightarrow j_f = 6$. The initial rotational state of $j_i = 12$ is first deexcited to the state of $j_i = 11$ in the same arrangement channel, and then the rearrangement occurs between $j_i = 11$ and $j_f = 6$ at the avoided crossing labeled A. The other would probably be $j_i = 12 \rightarrow j_f = 7 \rightarrow j_i = 11 \rightarrow j_f = 6$. These three transitions are dominated by the avoided crossings B, E, and A, respectively.

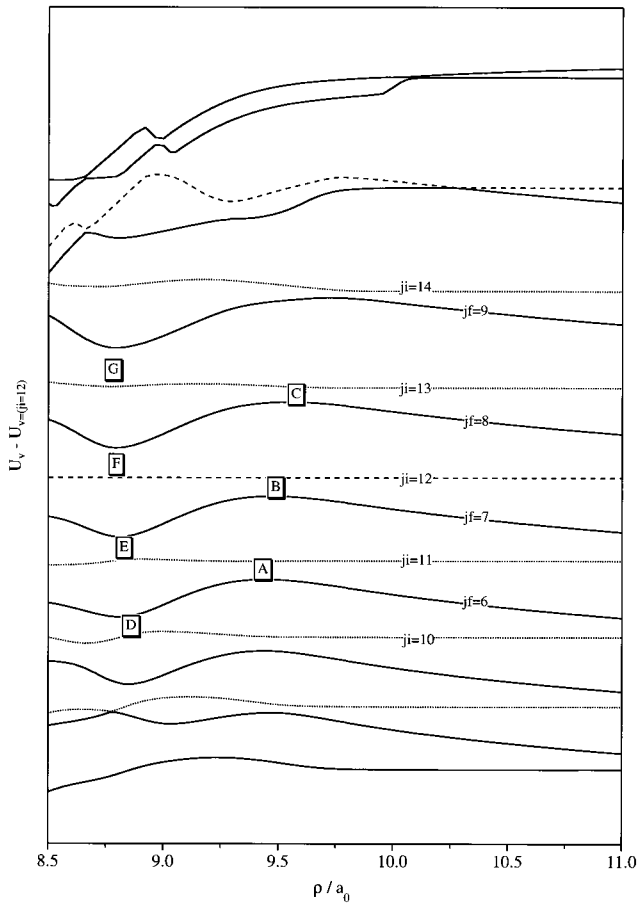

Figure 9. Small number of states around $j_i = 12$ measured from the latter. The alphabetical characters designate important avoided crossings.

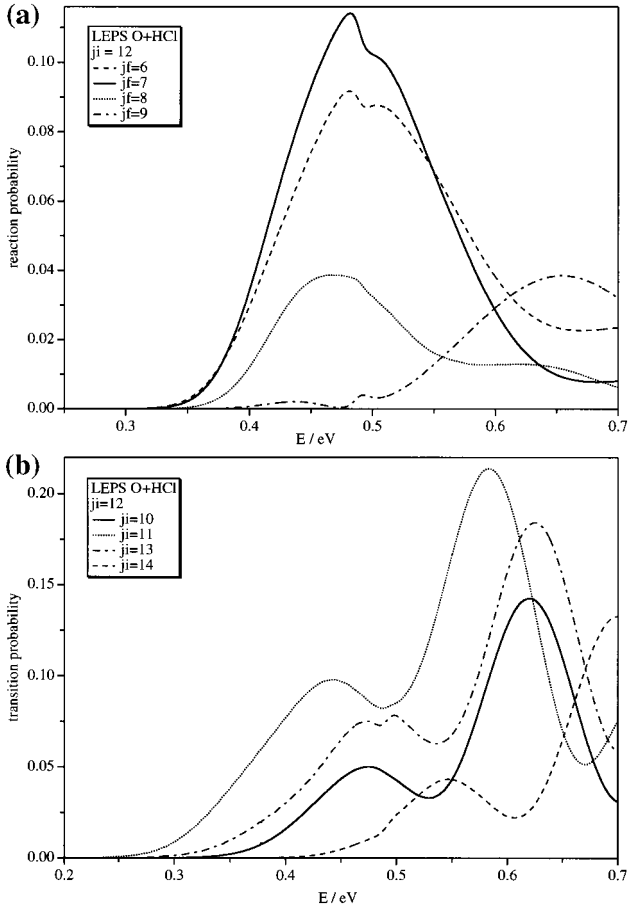

Figure 10. (a) State-to-sate reaction probabilities for $j_i = 12$ and j_f= 6−9 as a function of the total energy E in the case of LEPS of OHCl. (b) State-to-state nonreactive inelastic transition probabilities for j_i = $12 \rightarrow j_i = 10-14$ in the case of LEPS of OHCl.

The reaction probability for $j_i = 12 \rightarrow j_f = 8$ is less than one-half of the maximum peak of $j_f = 7$. This reaction at $E \lesssim$ 0.45 eV would be caused by the nonadiabatic transition at the avoided crossing labeled C through the inelastic transition between $j_i = 12$ and $j_i = 13$, which is less effective than that of $j_i = 12 \rightarrow j_i = 11$, as is shown in Figure 10b.

The reaction $j_i = 12 \rightarrow j_f = 9$ is not effective at $E \lesssim 0.5$ eV. This is simply because there is no effective path to connect these states.

So far, we have discussed only the rearrangement (reactive) transitions in terms of the nonadiabatic transitions at avoided crossings. Figure 10b shows some nonreactive inelastic transitions from $j_i = 12$. It should be noted that the deexcitation processes ($j_i = 12 \rightarrow j_i = 11$, 10) are more probable than the excitation processes ($j_i = 12 \rightarrow j_i = 13$, 14) and that the transitions by two quanta are less than those of one quantum. Although there are no clear avoided crossings among the potential curves belonging to the same arrangement channel, we can see some characteristic features about the inelastic transitions as a function of energy. Let us consider the inelastic transition $j_i = 12 \rightarrow j_i = 10$. The first peak at $E \approx 0.47$ eV could be assigned to $j_i = 12 \rightarrow j_i = 11 \rightarrow j_f = 6 \rightarrow j_i = 10$. Actually, the avoided crossing between $j_i = 10$ and $j_f = 6$ (labeled D) roughly corresponds to this peak position. Since this process competes with that of $j_i = 12 \rightarrow j_i = 11$, the first dip in the process of $j_i = 12 \rightarrow j_i = 11$ appears at almost the same energy as that of the above peak. All the above expectations have been confirmed by artificially cutting off the couplings between certain appropriate states, although the results are not shown here.

B. Cl + HCl. Full numerical calculations of this system are reported elsewhere.[23] Here, we concentrate on clarifying the mechanisms. Figure 11 shows vibrationally adiabatic cumulative reaction probabilities for $v_i = 0-3$. The onsets of the probability are naturally shifted to higher energies with increasing v_i. They are not equal to the energetic threshold but equal to the energy at which the corresponding potential ridge becomes available, although the difference between them becomes smaller as v_i increases. This confirms the significance of potential ridge lines.

Figures 12 and 13 depict some examples of state-to-state reaction probabilities, namely, for ($v_i = 0$, $j_i = 19$) → ($v_f = 1$, j_f) and ($v_i = 1$, $j_i = 18$) → ($v_f = 2$, j_f), respectively, together with the corresponding magnified adiabatic potential energy curve diagrams. As is clearly seen from these figures, the reactions proceed predominantly to particular final states, i.e., $j_f = 10$ in Figure 12 and $j_f = 8$ in Figure 13. These are due to the avoided crossings seen in the magnified potential curve diagrams. These transitions actually show up as peaks in the cumulative reaction probabilities (not shown here). Thus, as has been often claimed in the present series of studies, we can pick up some important avoided crossings that give rise to dominant state-to-state reactive transitions and can clarify the main reaction mechanisms.

5. Vibrational Effects on Potential Curve Splittings in Symmetric System

Figure 14 is a magnification of Figure 2 in the energy region $0.12 \lesssim E \lesssim 0.7$ eV. It is interesting to note the following

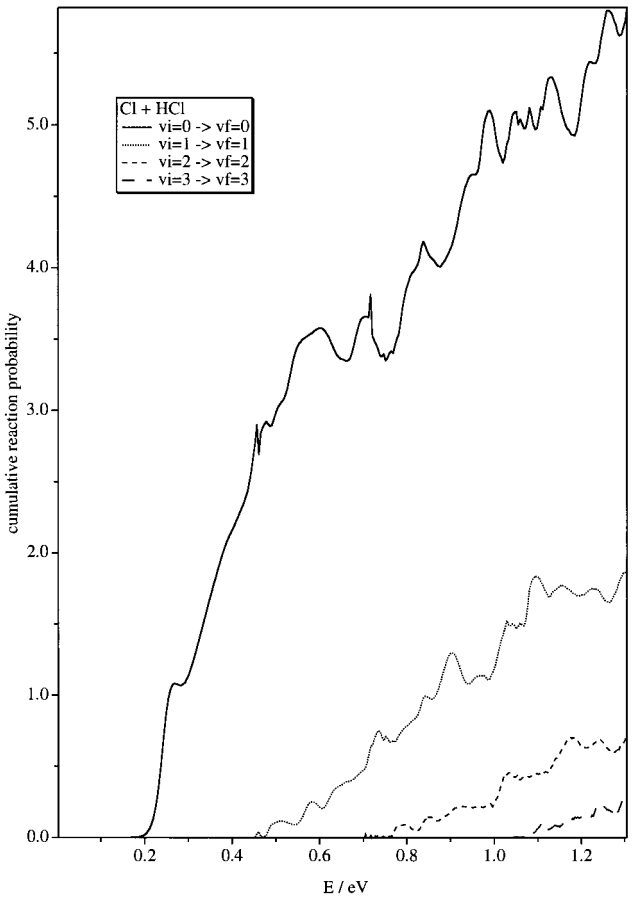

Figure 11. Vibrationally adiabatic cumulative reaction probabilities in the case of Cl + HCl.

features. At $0.2 \lesssim E \lesssim 0.45$ eV each potential curve splits into two (gerade and ungerade) curves at a position "a" slightly to the right of the $n_\xi = 0$ ridge line. At lower energies $E \lesssim 0.2$ eV no split is seen. These features can be understood easily because the potential ridge represents a potential barrier for reactive transition, tunneling through which gives rise to the energy splitting. This occurs at a slightly larger ρ than the potential ridge line. At low energies ($E \lesssim 0.2$ eV) the barrier is too high for the tunneling to occur effectively. Another interesting feature is that there are two groups of splittings ("a" and "b") at 0.45 eV $\lesssim E \lesssim$ 0.7 eV and that the splittings "b" at larger ρ to the right of the $n_\xi = 0$ ridge line correspond to the states asymptotically correlating to the $v = 1$, not $v = 0$, manifold. In other words, the splittings of the $v = 1$ states occur in front of the $n_\xi = 0$ ridge line and the splittings of the $v = 0$ states occur at smaller ρ in front of the $n_\xi = 1$ ridge line at "a". This is due to the vibrational nonadiabaticity in the η-space, as was discussed previously (see, for instance, Figure 5 of ref 11). Namely, vibrationally nonadiabatic transitions occur in the η-motion. Because of this nonadiabaticity, the $v = 1$ states feel the $n_\xi = 0$ potential barrier in the η-space as a reaction barrier. This switching or vibrational nonadiabaticity is reflected in the fact that the vibrationally nonadiabatic reactive transitions between these relevant pair of states occur effectively, as was demonstrated in the previous section. It should be noted that some peculiar attractive states (pendulum states)[6,11] appear where this switching occurs. It is interesting to note also that in this region there are some states that do not depict gerade and ungerade splittings as discussed also in ref 6. These features present intriguing subjects to be further investigated in connection also with the dynamical tunneling.[24]

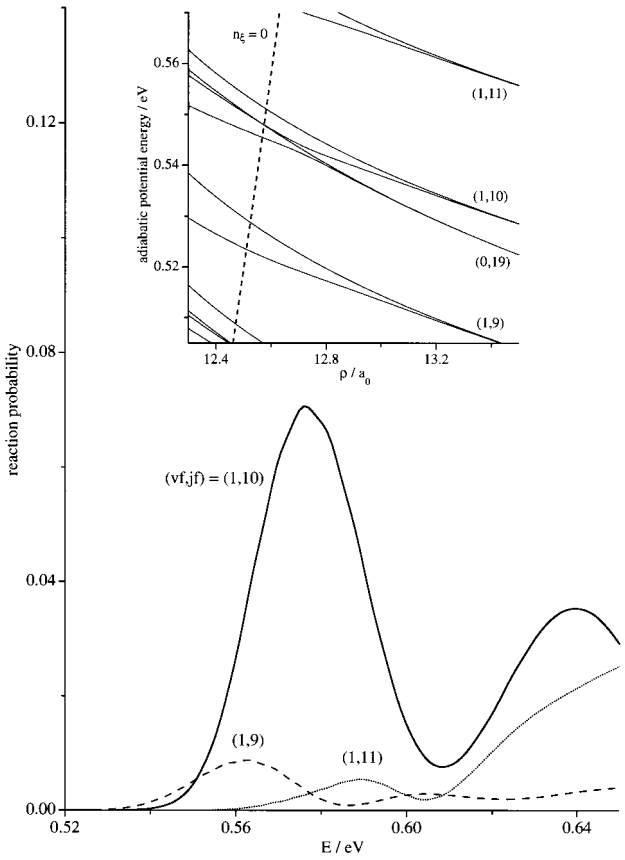

Figure 12. State-to-state reaction probabilities for Cl + HCl($v_i = 0$, $j_i = 19$) → HCl($v_f = 1$, j_f) + Cl as a function of total energy. Upper panel shows the magnification of the corresponding adiabatic potential energy curves around ($v_i = 0$, $j_i = 19$). The dash line in this panel represents the $n_\xi = 0$ ridge line.

6. Concluding Remarks

In the present series of work, we have planned not only to develop an efficient numerical method but also to elucidate mechanisms of heavy−light−heavy chemical reactions. In this paper we have proposed two, diabatic and adiabatic, decoupling procedures in order to reduce the number of states within the framework of the hyperspherical coordinate approach. To obtain a numerically converged **S** matrix in the close-coupling type computations in the total energy range studied here, 100−200 channels should usually be taken into account. We can easily expect, on the other hand, that only a limited number of states around any specified initial state would play a significant role in the reaction. This was actually confirmed in the present work. The diabatic decoupling procedure was shown to be useful for decoupling those channels or manifolds of states that sharply avoid crossing each other. The adiabatic decoupling scheme simply decouples those states that are adiabatically well separated from the central states. If two arrangement channels have quite different potential shapes and are well separated either by a potential barrier or by a dynamical barrier, the corresponding potential curves show sharp avoided crossings between the two groups. In such a case the diabatic decoupling scheme becomes very effective not only for numerical calculations but also for clarifying the mechanisms. This reduction of the number of states tells us that we can try to understand reaction mechanisms by considering only small number of states. In the case of HLH reactions, this clarification of mechanisms can be nicely done in terms of nonadiabatic transitions at important avoided crossings.

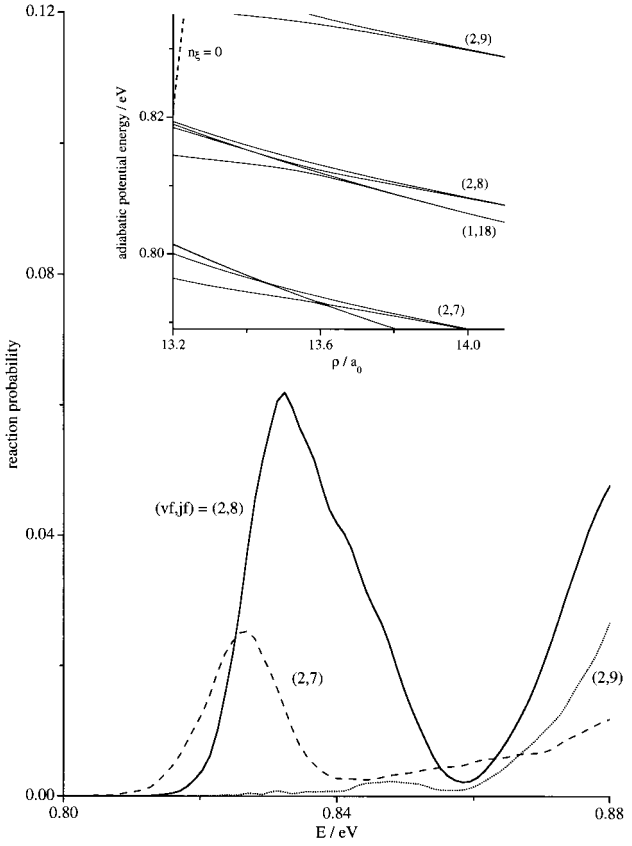

Figure 13. State-to-state reaction probabilities for Cl + HCl($v_i = 1$, $j_i = 18$) → HCl($v_f = 2$, j_f) + Cl as a function of total energy. Upper panel shows the magnification of the corresponding adiabatic potential energy curves around ($v_i = 1$, $j_i = 18$). The dash line in this panel represents the $n_\xi = 0$ ridge line.

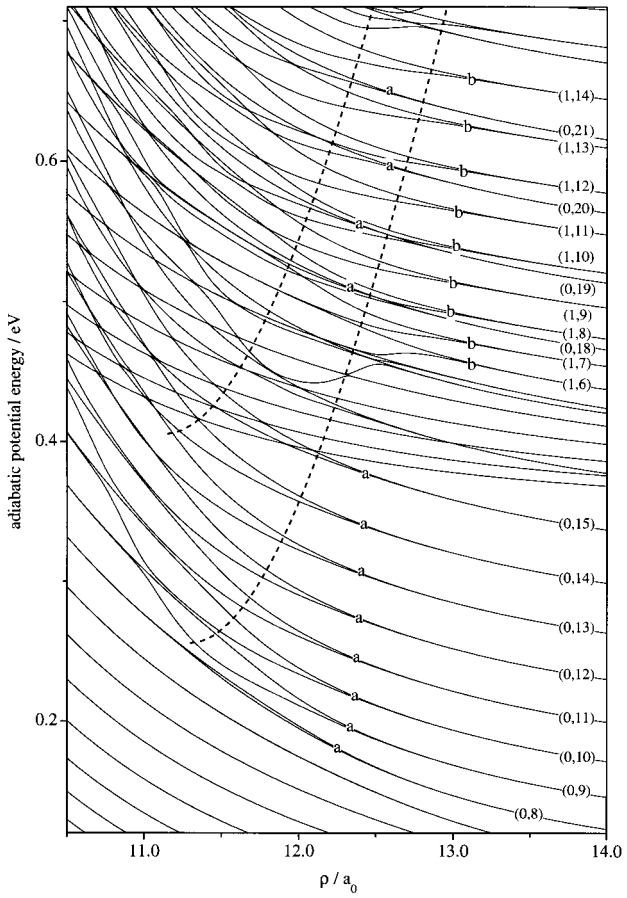

Figure 14. Magnification of Figure 2 in the energy region 0.12 eV ≲ E ≲ 0.7 eV.

The method was applied to a typical example of thermoneutral HLH reactions, i.e., O(^{3}P) + HCl → OH + Cl with use of both LEPS and KSG potentials, and also to an example of symmetric HLH reactions, Cl + HCl → HCl + Cl, with use of the LEPS potential. In all these cases the idea worked well to clarify the main mechanisms. Clarification of the mechanisms of asymmetric endo- or exothermic HLH reaction in terms of nonadiabatic transitions at avoided crossings will also be reported in a future publication.

Now, it is considered to be very natural to comprehend the HLH reactions in terms of vibrationally nonadiabatic transitions at avoided crossings. However, this has not been obvious at all before and becomes possible only with the help of the concept of potential ridge and the decoupling procedures introduced in the present series of works. In the present work we have mainly been concerned about the dynamics at low energies, i.e., at energies around the first peaks of reaction probabilities against energy. The dynamics at higher energies are controlled by transitions at ρ much smaller than the ridge lines and become more complicated, although they must be still dictated by avoided crossings there. In this sense, classification of the avoided crossings with respect to their significance in dynamics becomes more important. The criterion $O_{iv,j\mu} \geq$ CRT employed in the present work was demonstrated to be quite useful but is limited. The new analytical theory of nonadiabatic transitions at avoided crossings recently completed by Zhu and Nakamura[25−28] could be very effective for this. There are two basic parameters denoted a^2 and b^2 that characterize the nonadiabatic transitions.[25,26] In particular, the parameter a^2, which represents effectively the shape of the potentials and the coupling, can provide a good criterion for classifying avoided crossings. Actually, we have confirmed that the "important" avoided crossings and the "sharp" avoided crossings we have considered in the case of OHCl are all in the important intermediate range of a^2, which leads to sizable transition probabilities, and in the asymptotically large region, which corresponds to diabatic connection, respectively. Thus, the findings in the present work suggest that we might be able to analyze the heavy−light−heavy reactions by this new theory analytically and that we could obtain a further, deeper insight into the reaction mechanisms.

Acknowledgment. The present work was partly supported by a Grant-in-Aid for Scientific Research on Priority Area "Quantum Tunneling of Group of Atoms as Systems with Many Degrees of Freedom" and also by a Research Grant 10440179 from the Ministry of Education, Science, Culture and Sports of Japan. O.I.T. thanks the ministry for supporting him as a research fellow of the Institute for Molecular Science.

References and Notes

(1) *Theory of Chemical Reaction Dynamics*−; Baer, M., Ed.; CRC Press: Boca Raton, FL, 1985; Vols. I−IV.

(2) *Advances in Molecular Vibrations and Collision Dynamics*; Bowman, J. M., Ed.; JAI Press: Greenwich, 1994; Vols. 2A, 2B.

(3) *Dynamics of Molecules and Chemical Reactions*; Wyatt, R. E., Zhang, J. Z. H., Eds.; Marcel Dekker: New York, 1996; Vols. 1, 2.

(4) Schatz, G. C. *Chem. Phys. Lett.* **1988**, *151*, 409; *J. Chem. Phys.* **1989**, *90*, 3582; *J. Phys. Chem.* **1990**, *94*, 6157. Schatz, G. C.; Sokolovski, D.; Connor, J. N. L. *J. Chem. Phys.* **1991**, *94*, 4311. Connor, J. N. L.; McCabe, P.; Sokolovski, D.; Schatz, G. C. *Chem. Phys. Lett.* **1993**, *206*, 119. Schatz, G. C.; Sokolovski, D.; Connor, J. N. L. In *Advances in Molecular Vibrations and Collision Dynamics*; Bowman, J. M., Ed.; JAI Press: Greenwich, 1994; Vol. 2B, p 1. Sokolovski, D.; Connor, J. N. L.; Schatz, G. C. *J. Chem. Phys.* **1995**, *103*, 5979. Maierle, C. S.; Schatz, G.

C.; Gordon, M. S.; McCabe, P.; Connor, J. N. L. *J. Chem. Soc., Farady Trans.* **1997**, *93*, 709.

(5) Koizumi, H.; Schatz, G. C.; Gordon, M. S. *J. Chem. Phys.* **1991**, *95*, 6421.

(6) Rougeau, N.; Kubach, C. *Chem. Phys.* **1993**, *175*, 299. Vien, G. N.; Rougeau, N.; Kubach, C. *Chem. Phys. Lett*. **1993**, *215*, 35. Rougeau, N.; Kubach, C. *Chem. Phys. Lett*. **1994**, *228*, 207. Vien, G. N.; Kubach, C. *Chem. Phys.* **1994**, *179*, 131. Rougeau, N.; Kubach, C. *J. Mol. Struct.: THEOCHEM* **1995**, *330*, 57; *Chem. Phys. Lett*. **1997**, *274*, 535.

(7) Skodje, R. T. *J. Chem. Phys.* **1991**, *95*, 7234. Grayce, B. B.; Skodje, R. T. *J. Chem. Phys.* **1991**, *95*, 7249; *J. Phys. Chem*. **1992**, *96*, 4134. Grayce, B. B.; Skodje, R. T.; Hutson, J. M. *J. Chem. Phys*. **1993**, *98*, 3929.

(8) Moribayashi, K.; Nakamura, H. *J. Phys. Chem.* **1995**, *99*, 15410. Tsuda, K.; Moribayashi, K.; Nakamura, H. *J. Chem. Phys*. **1995**, *103*, 5512. Nobusada, K.; Moribayashi, K.; Nakamura, H. *J. Chem. Soc., Faraday Trans*. **1997**, *93*, 721.

(9) Thompson, W. H.; Miller, W. H. *J. Chem. Phys.* **1997**, *106*, 142.

(10) Poirier, B. *J. Chem. Phys.* **1998**, *108*, 5216.

(11) Tolstikhin, O. I.; Nakamura, H. *J. Chem. Phys.* **1998**, *108*, 8899.

(12) Nobusada, K.; Tolstikhin, O. I.; Nakamura, H. *J. Chem. Phys.* **1998**, *108*, 8922 (referred to as I).

(13) Tolstikhin, O. I.; Watanabe, S.; Matsuzawa, M. *Phys. Rev. Lett*. **1995**, *74*, 3573.

(14) Tolstikhin, O. I.; Watanabe, S.; Matsuzawa, M. *J. Phys. B.* **1996**, *29*, L389.

(15) Light, J. C.; Hamilton, I. P.; Lill, J. V. *J. Chem. Phys.* **1985**, *82*, 1400.

(16) Fano, U. *Phys. Rev. A* **1981**, *24*, 2402; *Prog. Phys.* **1983**, *46*, 97.

(17) Aquilanti, V.; Grossi, G.; Lagana, A. *Chem. Phys. Lett*. **1982**, *93*, 174; *Chem. Phys. Lett*. **1982** *93*, 179. Aquilanti, V.; Cavalli, S.; Grossi, G.; Lagana, A. *J. Mol. Struct.* **1984**, *107*, 95. Aquilanti, V.; Cavalli, S.; Grossi, G. *Chem. Phys. Lett.* **1984**, *110*, 43. Aquilanti, V.; Cavalli, S. *Chem. Phys. Lett.* **1987**, *141*, 309. Aquilanti, V. In *The Theory of Chemical Reaction Dynamics*; Clary, D. C., Ed.; Reidel: Dordrecht, 1986; p 383.

(18) Ohsaki, A.; Nakamura, H. *Phys. Rep*. **1990**, *187*, 1.

(19) Baluja, K. L.; Burke, P. G.; Morgan, L. A. *Comput. Phys. Comm.* **1982**, *27*, 299.

(20) Persky, A.; Broida, M. *J. Chem. Phys.* **1984**, *81*, 4352.

(21) Bondi, D. K.; Connor, J. N. L.; Manz, J.; Römelt, J. *Mol. Phys.* **1983**, *50*, 467.

(22) Ramachandran, B.; Senekowitsch, J.; Wyatt, R. E. J. *Mol. Struct.: THEOCHEM* **1996**, *388*, 57.

(23) Nobusada, K.; Tolstikhin, O. I.; Nakamura, H. *J. Mol. Struct.: THEOCHEM*, in press.

(24) Hashimoto, N.; Takatsuka, K. *J. Chem. Phys.* **1998**, *108*, 1893.

(25) Nakamura, H. In *Dynamics of Molecules and Chemical Reacrions*; Wyatt, R. E., Zhang, J. Z. H., Eds.; Marcel Dekker: New York, 1996; p 473.

(26) Nakamura, H.; Zhu, C. *Comments At. Mol. Phys.* **1996**, *32*, 249.

(27) Nakamura, H. *Annu. Rev. Phys. Chem.* **1997**, *48*, 299.

(28) Zhu, C.; Nakamura, H. *J. Chem. Phys.* **1998**, *108*, 7501.